4973

Diffusion-weighted magnetic resonance spectroscopy in the cerebellum of a rat model of hepatic encephalopathy at 14.1T

Jessie Mosso[1,2,3], Julien Valette[4], Katarzyna Pierzchala[1,2], Dunja Simicic[1,2,3], Ileana Ozana Jelescu[1,2], and Cristina Cudalbu[1,2]
[1]CIBM Center for Biomedical Imaging, Lausanne, Switzerland, [2]Animal Imaging and Technology, EPFL, Lausanne, Switzerland, [3]LIFMET, EPFL, Lausanne, Switzerland, [4]Commissariat à l'Energie Atomique (CEA), Institut d'Imagerie Biomédicale (I2BM), Molecular Imaging Research Center (MIRCen), Fontenay-aux-Roses, France

Synopsis

Chronic hepatic encephalopathy (cHE) is a severe brain condition arising from chronic liver disease. Microstructural changes occurring due to toxins accumulation in the brain are still unexplored *in vivo*, especially in cerebellum, and of key interest for disease early detection. Using the STE-LASER sequence, we measured a decreased diffusion coefficient for glutamine and increased for taurine and glutamate in the cerebellum of a rat model of cHE, associated with cell-specific morphological changes measured *ex vivo*. These preliminary results need to be confirmed by increasing the sample size but they shed light on new aspects in the pathophysiology of HE.

Introduction

Chronic hepatic encephalopathy (cHE) is a severe brain condition arising from chronic liver disease (CLD) and leading to irreversible cognitive and neurological damage. The diseased liver fails to clear toxins from blood, leading to hyperammonemia[1], brain glutamine (Gln) excess[2] and osmotic imbalance. Yet, the field lacks *in vivo* and non-invasive studies on brain microstructural changes associated to this load of toxins to better target treatments. Diffusion-weighted magnetic resonance spectroscopy (DW MRS) holds this promise, allowing to extract cell-specific information on metabolites compartmentation (Gln, Ins astrocytic and Glu, NAA neuronal metabolites) and tissue microstructure. In a rat model of cHE, the bile duct ligated (BDL) rat, the cerebellum shows stronger neurometabolic changes (Gln increase and osmotic response[3]) than the hippocampus and striatum but remains a challenging region for MRS investigation. The aim of the present work was to investigate for the first time the metabolites diffusion properties in the cerebellum in a rat model of cHE at ultra-high field (14.1T), using the STE-LASER[4] sequence, and to link them to astrocytic and neuronal microstructural changes observed by histological measures.

Methods

The BDL rat model for CLD-induced HE[5] was used (n=3 BDL, n=4 Sham). Plasma bilirubin and ammonium were measured longitudinally. Both groups were scanned 6 weeks post-surgery on a 14.1T scanner (Bruker/Magnex Scientific), using the STE-LASER[4] sequence with respiratory triggering and strict monitoring of breathing rate (65resp/min) and temperature (37.7°). A homemade transmit/receive quadrature surface coil was positioned above the cerebellum (voxel: 30-78.4µL). The parameters used are described in Fig 1. Prior to quantification with LCModel, spectra for each b-value were corrected for eddy currents, B0 drift, and phase distortions between blocks of 8 repetitions, and quality control at each b-value based on relative CRBs (<40%) was applied. A metabolite basis set was simulated with NMRSCOPE-B from jMRUI, including an *in vivo* macromolecule spectrum. Metabolite signals were normalized to one at the smallest b-value before averaging. A linear model was fitted to the log of the normalized decays up to b=5ms/µm^2, while a model of randomly oriented sticks[6] $S = S_0\sqrt{\frac{\pi}{4bD_{intra}}}erf(\sqrt{bD_{intra}})$ was fitted to the normalized decays up to b=15ms/µm2. Immunohistochemistry (IHC) and Golgi-Cox stainings were performed for cerebellar astrocytes and neurons cytoarchitecture. IHC: 16µm brain sagittal-sections, GFAP (glia-specific intermediate-filament protein) and DAPI (nucleus) stainings were used (seven slides/rat). Morphometric measurements were performed using Sholl-analysis (~1000 processes/group/region).Golgi-Cox: metallic impregnation of neurons (110µm-sagittal-sections, 25-slides/hemisphere).

Results and discussion

BDL rats showed the typical changes related to cHE, confirming the disease progression: increased blood bilirubin (from <0.5 mg/dl to 7.8 +/- 0.8 mg/dl) and ammonium (from 16.5 to 55.3 +/- 5.1 µmol/l) together with increased brain Gln (+71%) and decreased main organic osmolytes (Ins, Tau, tCho, -9%, -14%, -21%) measured with a STEAM sequence (Fig 2A). Fig 2B shows representative diffusion sets for both groups. The signal decay of Glu, Ins, NAA, Glx, tCho, tCr, showed a similar trend between both groups (non-significant difference), whereas Gln signal decay was slower (p=0.04) and Tau signal decay was faster (p=0.05) for BDL compared to Sham rats (Fig 2C). The apparent diffusion coefficients (ADC) fitted with a linear model up to b=5ms/µm^2 are in good agreement with literature[7] (Fig 3, top left). Although few data points were used at b=15ms/µm2 for the stick model (Fig 3, bottom left: n=1 Sham, n=1 BDL), both fits yield similar trends. The ADC (resp. D_{intra}) increased (significant for Tau and Glu) in BDL rats compared to Sham rats for all metabolites except for Gln, where the ADC (resp. D_{intra}) decreased (Fig 3, right). These trends also reflect previous DW-MRS work[8] on a voxel positioned in the center of the brain at 9.4T, except for Gln where no difference had been observed, confirming its stronger effect on the cerebellum. A significant increase in GFAP+ cells and nuclei was observed for cerebellar protoplasmic astrocytes (+21%, p**), suggesting an astrocytic activation, together with a significant decrease of the number of processes (-41%, p***) and of the mean length of intermediate filaments (-35%, p*) in the granular layer. Golgi-Cox staining of Purkinje cells showed a significant decrease of the neuronal soma surface (-22%, p***) and dendritic spines density (-24%, apical, p***). It has been suggested, based on numerical simulations[9], that a decrease in dendritic spine density would increase the ADC for neuronal metabolites (NAA, Glu), which is consistent with our DW-MRS and histological results. Gln, an astrocytic metabolite, showed an ADC decrease for BDL that can be associated with shorter astrocyte processes, as well as increased complexity of Bergmann glia fibers. Additionally, Gln transporters (SNAT 5) are down regulated in HE[10], blocking Gln clearance from astrocytes. This could be reflected in the difference in diffusion patterns between Gln and other astrocytic metabolites (Ins, tCho), the later leaking in the extracellular space to preserve osmotic balance and being cleared out from the brain. Overall these preliminary results showed that HE leads to profound microstructural alterations of both neurons and astrocytes in cerebellum probed *in vivo* using DW-MRS and confirmed by histological measures. Further analysis will require an increased number of spectra at high b-values and samples together with improvements in the SNR by optimizing the voxel size and exploring noise reduction techniques.

Acknowledgements

Supported by the SNSF project no 310030_173222 and the European Union's Horizon 2020 research and innovation program under the Marie Sklodowska-Curie grant agreement No 813120 (INSPiRE-MED). We acknowledge access to the facilities and expertise of the CIBM Center for Biomedical Imaging, a Swiss research center of excellence founded and supported by Lausanne University Hospital (CHUV), University of Lausanne (UNIL), Ecole

polytechnique fédérale de Lausanne (EPFL), University of Geneva (UNIGE) and Geneva University Hospitals (HUG). We thank Stefanita Mitrea and Dario Sessa for the BDL surgeries and veterinary support.

References

1. Tranah, T. H., Vijay, G. K. M., Ryan, J. M. & Shawcross, D. L. Systemic inflammation and ammonia in hepatic encephalopathy. Metab Brain Dis 28, 1–5 (2013).

2. Braissant, O. et al. Longitudinal neurometabolic changes in the hippocampus of a rat model of chronic hepatic encephalopathy. J. Hepatol. 71, 505–515 (2019).

3. Simicic, D. et al. P: 33 In Vivo Longitudinal 1H MRS Study of Hippocampal, Cereberal and Striatal Metabolic Changes in the Adult Brain Using an Animal Model of Chronic Hepatic Encephalopathy. The American Journal of Gastroenterology 114, S17 (2019).

4. Ligneul, C., Palombo, M. & Valette, J. Metabolite diffusion up to very high b in the mouse brain in vivo: Revisiting the potential correlation between relaxation and diffusion properties. Magnetic Resonance in Medicine 77, 1390–1398 (2017).

5. Butterworth, R. F. et al. Experimental models of hepatic encephalopathy: ISHEN guidelines. Liver International 29, 783–788 (2009).

6. Callaghan, P. T. Principles of Nuclear Magnetic Resonance Microscopy. (Clarendon Press, 1993).

7. Ligneul, C. et al. Diffusion-weighted magnetic resonance spectroscopy enables cell-specific monitoring of astrocyte reactivity in vivo. NeuroImage 191, 457–469 (2019).

8. Cudalbu, C. et al. Diffusion of brain metabolites highlights altered brain microstructure in chronic hepatic encephalopathy. in Proc. Intl. Soc. Mag. Reson. Med. 28 (2020).

9. Palombo, M., Ligneul, C., Hernandez-Garzon, E. & Valette, J. Can we detect the effect of spines and leaflets on the diffusion of brain intracellular metabolites? NeuroImage 182, 283–293 (2018).

10. Desjardins, P., Du, T., Jiang, W., Peng, L. & Butterworth, R. F. Pathogenesis of hepatic encephalopathy and brain edema in acute liver failure: role of glutamine redefined. Neurochem Int 60, 690–696 (2012).

Figures

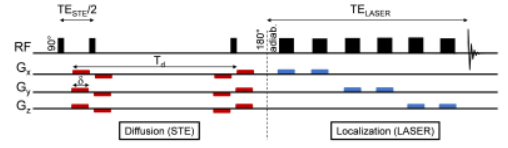

TE_{STE}(ms)	TE_{LASER}(ms)	TR(ms)	δ(ms)	T_d(ms)
8.7	25	2000	3	63.4

b values(ms/μm²)	0.05	0.5	1	3	5	15
Repetitions	320	320	320	320	320	608

A. Schematic representation of the STE-LASER[4] sequence with relevant acquisition parameters. Black: RF pulses, red: bipolar diffusion gradients, blue: localization gradients. For clarity, spoiler gradients are not shown. δ: duration of diffusion gradients, T_d: diffusion time.

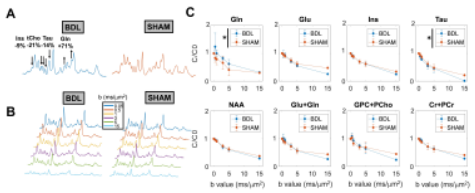

A. Representative neurometabolic profiles in BDL and Sham rats acquired at 14.1T in the cerebellum (STEAM sequence - TE=3ms, TM=10ms, LB=8Hz) B. Representative spectra at different b-values for BDL and SHAM rats acquired with the STE-LASER[4] sequence (LB=8Hz) in the cerebellum at 14.1T. C. Individual metabolite decays versus b-values for both groups. Error bars: dispersion around the mean value. Statistics: 2-way ANOVA with variables disease and b-value, *: p<0.05.

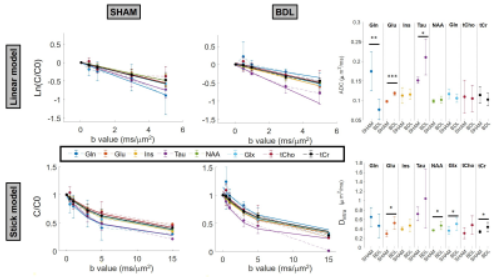

Left: fit of metabolite signal decays in both groups: mono-exponential fit up to b=5ms/μm^2 (top), stick model fit up to b=15ms/μm^2 (bottom), Glu+Gln=Glx, GPC+PCho=tCho, Cr+PCr=tCr. Error bars: dispersion around the mean. Right: corresponding ADC and Dintra. Error bars: standard deviation from Monte Carlo simulations (noise: standard deviation in the difference between mean and best fit). T-test between the mean ADC or D_{intra} between groups for each metabolite: * p<0.05, ** p<0.01, *** p<0.001.

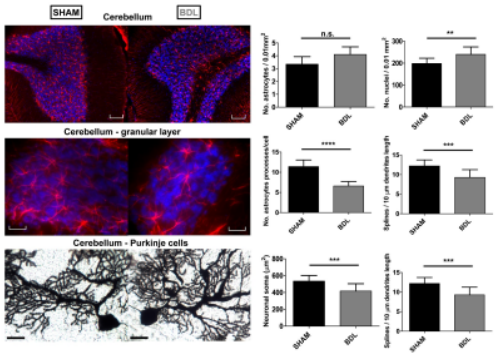

IHC staining in the cerebellum of Sham and BDL rats. Top: anti-GFAP(red)/DAPI(blue) staining of the cerebellar folium, scale bar: 100μm. Middle: GFAP/DAPI staining of the granular layer, scale bar: 25μm. Bottom: Colgi-Cox staining of Purkinje cells, scale bar: 25μm Right: corresponding quantifications, ** p<0.01, *** p<0.001, **** p<0.0001.

Abstract 0342

Figure 1

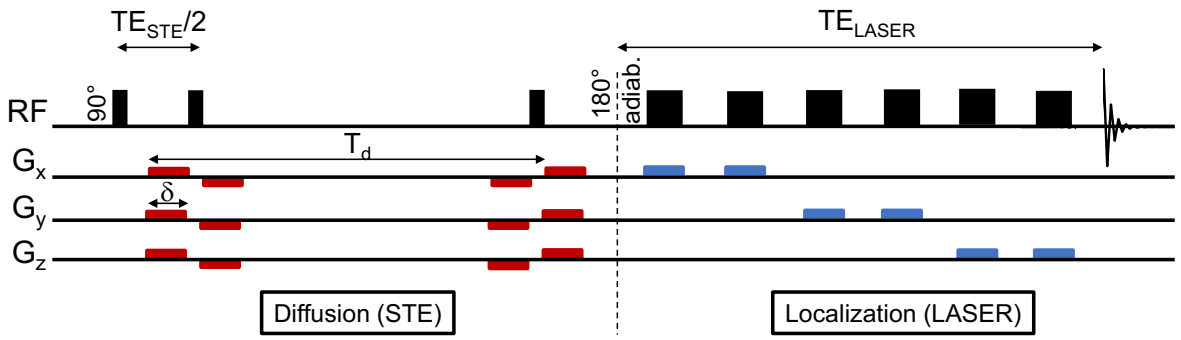

TE_{STE}(ms)	TE_{LASER}(ms)	TR(ms)	δ(ms)	T_d(ms)
8.7	25	2000	3	63.4

b values(ms/μm²)	0.05	0.5	1	3	5	15
Repetitions	320	320	320	320	320	608

Legend: A. Schematic representation of the STE-LASER[4] sequence with relevant acquisition parameters. Black: RF pulses, red: bipolar diffusion gradients, blue: localization gradients. For clarity, spoiler gradients are not shown. δ: duration of diffusion gradients, T_d: diffusion time.

Figure 2

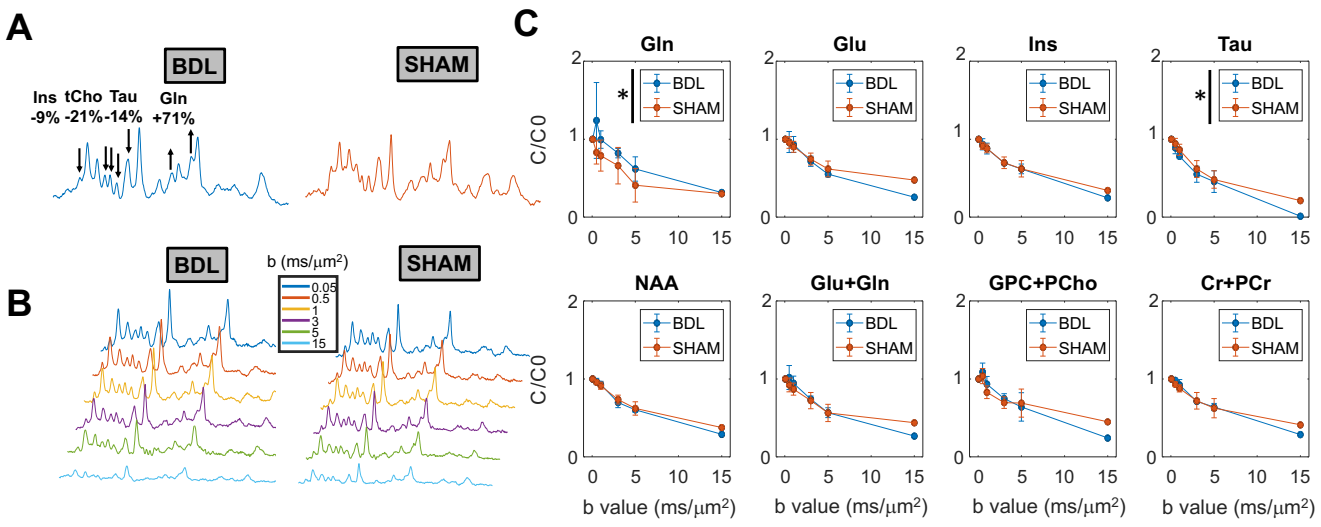

Legend: A. Representative neurometabolic profiles in BDL and Sham rats acquired at 14.1T in the cerebellum (STEAM sequence - TE=3ms, TM=10ms, LB=8Hz) B. Representative spectra at different b-values for BDL and SHAM rats acquired with the STE-LASER[4] sequence (LB=8Hz) in the cerebellum at 14.1T. C. Individual metabolite decays versus b-values for both groups. Error bars: dispersion around the mean value. Statistics: 2-way ANOVA with variables disease and b-value, *: p<0.05.

Figure 3

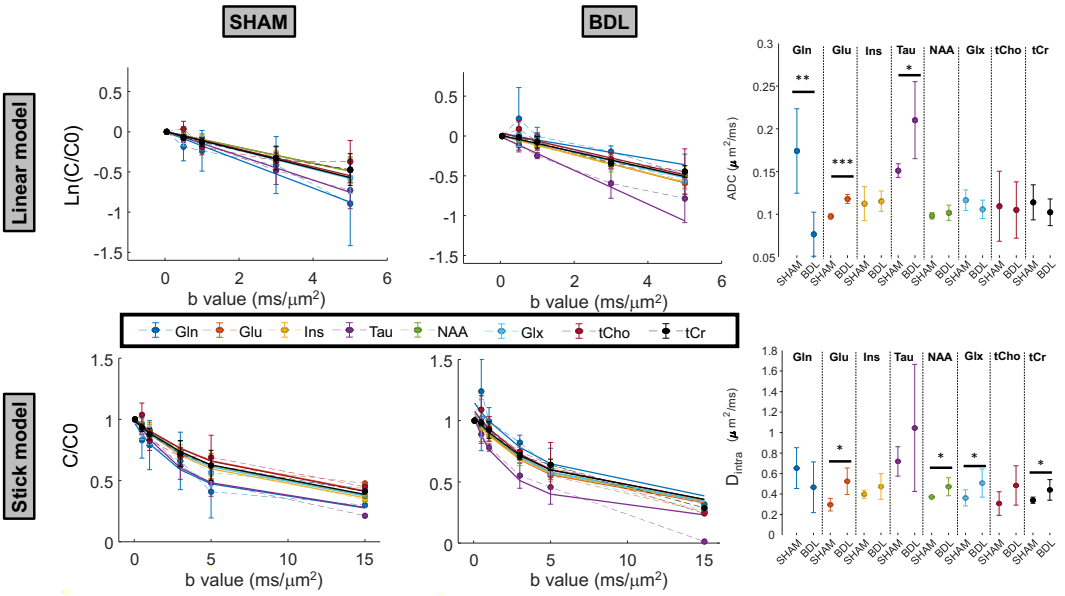

Legend: Left: fit of metabolite signal decays in both groups: mono-exponential fit up to b=5ms/μm^2 (top), stick model fit up to b=15ms/μm^2 (bottom), Glu+Gln=Glx, GPC+PCho=tCho, Cr+PCr=tCr. Error bars: dispersion around the mean. Right: corresponding ADC and Dintra. Error bars: standard deviation from Monte Carlo simulations (noise: standard deviation in the difference between mean and best fit). T-test between the mean ADC or D_{intra} between groups for each metabolite: * p<0.05, ** p<0.01, *** p<0.001.

Figure 4

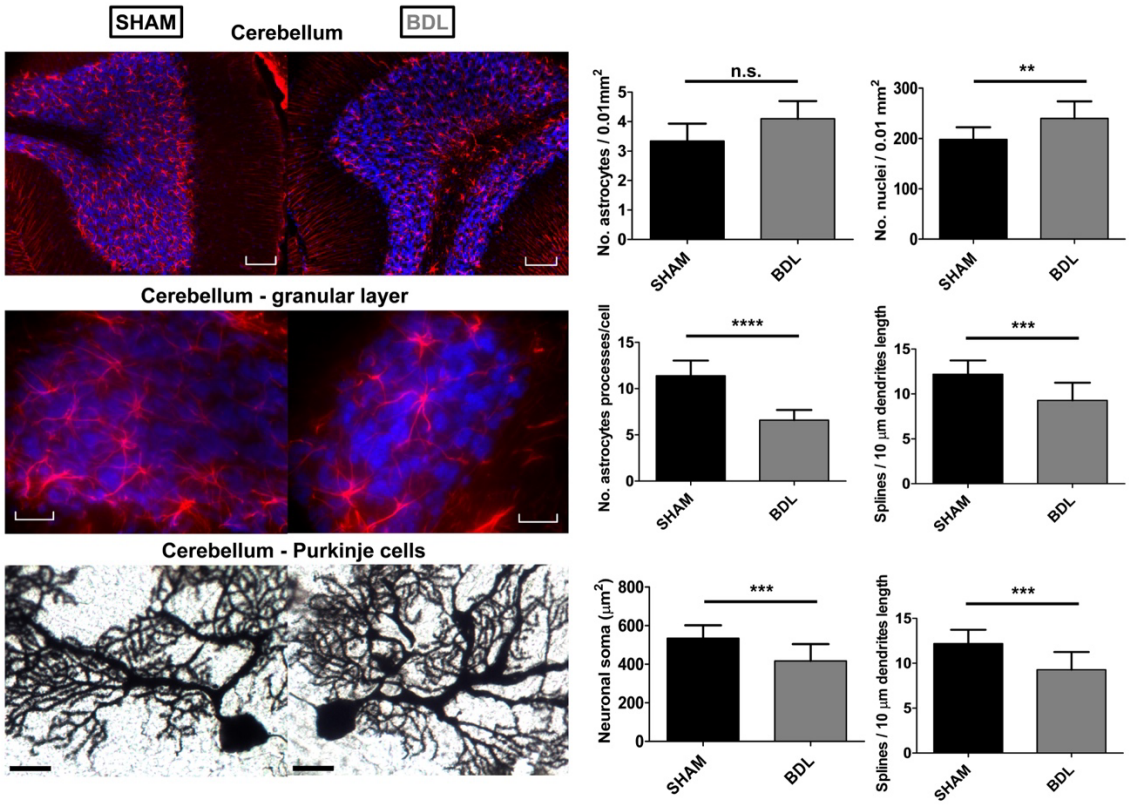

Legend: IHC staining in the cerebellum of Sham and BDL rats. Top: anti-GFAP(red)/DAPI(blue) staining of the cerebellar folium, scale bar: 100μm. Middle: GFAP/DAPI staining of the granular layer, scale bar: 25μm. Bottom: Colgi-Cox staining of Purkinje cells, scale bar: 25μm Right: corresponding quantifications, ** p<0.01, *** p<0.001, **** p<0.0001.

References: 4. Ligneul, C., Palombo, M. & Valette, J. Metabolite diffusion up to very high b in the mouse brain in vivo: Revisiting the potential correlation between relaxation and diffusion properties. Magnetic Resonance in Medicine 77, 1390–1398 (2017).